Coordination Chemistry Reviews 253 (2009) 594–605

Contents lists available at ScienceDirect

Coordination Chemistry Reviews

journal homepage: www.elsevier.com/locate/ccr

Review

# First principles calculation of Mössbauer isomer shift

Michael Filatov

*Theoretical Chemistry, Zernike Institute for Advanced Materials, Rijksuniversiteit Groningen, Nijenborgh 4, 9747 AG Groningen, The Netherlands*

**Contents**



ARTICLE INFO

*Article history:*
Received 14 March 2008
Accepted 7 May 2008
Available online 14 May 2008

*Keywords:*
Mössbauer spectroscopy
Isomer shift
Contact density
Relativistic effects
Electronic structure calculations

ABSTRACT

Mössbauer spectroscopy is a widely used analytic tool which provides information about local electronic structure of solid materials on an atomic scale. The isomer shift of resonance nuclear γ transition is a sensitive parameter which depends on the charge and spin state of the resonating atom as well as on its chemical environment. Theory underlying the isomer shift is reviewed and its connection to the local electronic structure is discussed. A review of advances made in the *ab initio* calculation of isomer shift is presented. The importance of careful calibration of the parameters of nuclear γ transitions on the basis of high-level quantum chemical calculations with the inclusion of both relativistic effects and electron correlation is underlined. With the help of accurate theoretical calculations of the isomer shift over a wide range of chemical environments deeper understanding of a relationship between the observed spectroscopic parameters and the electronic structure of materials will be gained.



## 1. Introduction

Mössbauer or nuclear γ-resonance spectroscopy represents one of the fascinating techniques in modern chemical physics. After the discovery, in 1957, by Mössbauer [1] the resonance absorption of γ rays by the atomic nuclei, in only a few years, has established itself as one of the most powerful analytic techniques in chemistry and physics [2–16].

Currently, Mössbauer spectroscopy is a widely used technique of characterization for samples rich in iron and a large number of other isotopes. Besides iron $^{57}$Fe the Mössbauer effect is observed for more than 40 other elements in the periodic table, including elements such as tin, gold, mercury, uranium, rare earth elements, etc. [4–7,9]. Thus, Mössbauer spectroscopy enables one to study systematically and rapidly different charge and spin states of these elements as well as variations in the crystalline or chemical environment around them. The use of synchrotron γ-radiation in nuclear resonance scattering spectroscopies [17–23] enables determination of Mössbauer nuclei in very

*E-mail address:* m.filatov@rug.nl.

0010-8545/$ – see front matter © 2008 Elsevier B.V. All rights reserved.
doi:10.1016/j.ccr.2008.05.002

low concentrations thus extending the range of applicability of the method.

An important advantage of Mössbauer spectroscopy (and related spectroscopic techniques [17–24]) is that it is capable to provide information on the local electronic structure and chemical bonding on an atomic scale. Therefore, Mössbauer spectroscopy finds a large and increasing number of applications for the study of not only crystalline solids, but also of biological systems [11,12], molecules isolated in inert gas matrices [25–33], disordered solids [34–36], etc. The range of applications of Mössbauer spectroscopy varies from traditional solid-state physics and chemistry to biochemistry [11,12], nano-science [13] and materials science [8,34], to metallurgy [14,15] and even to space exploration studies [16].

Mössabuer spectroscopy is based on the phenomenon of recoilless resonance absorption of γ-rays by the atomic nuclei immersed in a crystalline or disordered solid environment [2,3,6]. The frequency of the nuclear γ transition depends on the interaction with the surrounding electrons and is thus influenced by the local electronic structure and chemical environment of the resonating atom. This makes the parameters of Mössbauer spectra, such as the isomer shift of the γ transition, the quadrupole splitting and the hyperfine splitting, sensitive characteristics of the electronic structure [4–7].

The Mössbauer isomer shift δ arises from the electrostatic interaction between nuclear and electron charge distributions due to the finite size of the nucleus [6,40,37–39]. When an atomic nucleus undergoes a γ transition, the size of the nucleus, as characterized by its charge radius and matter radius, changes and this leads to slightly different electron–nuclear interaction energies in the ground and in the excited states of the nucleus [40]. This energy difference is thus dependent on the local electronic structure. The isomer shift δ is defined as a measure of the energy difference between the energies of γ transitions occurring in the sample (absorber) nucleus as compared to the reference (source) nucleus. Because the electronic environments in which the sample and the reference nuclei are immersed are different, the isomer shift probes this difference.

However, the relationship between the isomer shift and the local electronic structure is by no means straightforward. Magnitude of the isomer shift is determined simultaneously by characteristics of the nuclear structure, such as the charge radius variation during the γ transition, and of the local electronic structure, such as the electron density in the vicinity of nucleus [6,40]. Although, in principle, both characteristics are physical observables, none of them is accessible via direct experimental measurements. In such a situation, the first principles quantum chemical calculations of the local electronic structure and of the isomer shift are of the utmost importance.

In the field of quantum chemical modeling of the isomer shift, there are several aspects which need to be addressed very carefully. First of all, the parameters of nuclear γ transitions must be accurately determined to allow a reliable conversion between the observed isomer shifts and parameters of the local electronic structure. Currently, the most accurate way of calibration of the nuclear γ transition parameters is via high-level *ab initio* electronic structure calculations. In these calculations, all relevant effects, such as the effects of relativity, the effects of electron correlation and of the solid-state environment, have to be included, which makes such calculations very demanding. Second, the relationship between the Mössbauer spectroscopy parameters and the local electronic structure need to be carefully studied. The knowledge of this relationship will enable one to analyze how the changes in local chemical environment influence the observed parameters of Mössbauer spectra. High-quality quantum chemical calculations are indispensable to address both these issues. Modeling of the observed spectroscopy parameters, such as the isomer shift, by *ab initio* calculations over a wide range of chemical environments and comparison with the experimental observations is a viable route for the further development of Mössbauer spectroscopy into an even more accurate technique of investigation of solid systems.

The present article addresses the aforementioned points important for theoretical modeling of the Mössbauer isomer shift. The theory of the isomer shift is outlined in Section 2 including the traditional approach based on the perturbational treatment of the electron–nuclear interactions (Section 2.1) and a recently suggested approach based on the direct calculation of the isomer shift (Section 2.3). The issue of calibration of the parameters of nuclear γ transitions is addressed in Section 3 and, in Section 4, the current status of the first principles calculations of isomer shift is reviewed.

## 2. Theory of Mössbauer isomer shift

Isomer shift in Mössbauer spectroscopy originates in the Coulomb interaction between nuclear and electronic charge distributions [3,7,6,39]. The interaction energy between the total electronic charge distribution $\rho(\mathbf{r})$ and the electrostatic potential $V_{\mathrm{Ne}}(\mathbf{r})$ generated by charged nucleons is given by

$$E_{\mathrm{Ne}} = \int \rho(\mathbf{r})\, V_{\mathrm{Ne}}(\mathbf{r})\, \mathrm{d}\mathbf{r} \tag{1}$$

For a point-charge nucleus, the electrostatic potential is $V_{\mathrm{Ne}}(\mathbf{r}) = -(Z/r)$ and the electron–nuclear interaction energy depends on the charge of the nucleus $Z$ only. If nucleus were a point-charge, then the interaction energy would be the same for the ground and the excited states of the nucleus. The electron–nuclear interaction would then generate a constant shift of the nuclear energy levels and there would be no isomer shift observed in Mössbauer experiments.

However, real nuclei have a finite size. The size of a real nucleus changes when the nucleus undergoes γ transition [3,39–42]. The electron–nuclear attraction potential $V_{\mathrm{Ne}}(\mathbf{r})$ changes with the nuclear size and the interaction energy between the nuclear charge distribution and the electron charge distribution is different in the ground and in the excited states of the nucleus. Thus, there appears a dependence of the energy of resonance γ quantum on the electronic environment, in which the given nucleus is immersed. Because in a Mössbauer experiment one measures the change of the energy of the resonance γ quantum between the source ($s$) and the absorber ($a$) nuclei, the isomer shift δ will be observed, which, in terms of the Doppler velocity necessary to achieve the resonance absorption (usually expressed in mm/s), is given in Eq. (2)[6,40]:

$$\delta = \frac{c}{E_\gamma}(\Delta E_\gamma^{\mathrm{a}} - \Delta E_\gamma^{\mathrm{s}}) \tag{2}$$

where $c$ is the velocity of light and $E_\gamma$ is the energy of the γ quantum, $E_\gamma \gg \Delta E_\gamma^{\mathrm{a}}, \Delta E_\gamma^{\mathrm{s}}$.

### 2.1. Perturbational approach to isomer shift

Traditionally, the energy differences $\Delta E_\gamma^{\mathrm{a,s}}$ are calculated within the framework of perturbation theory, whereby the variation of the electron–nuclear interaction potential is treated as a weak perturbation of the nuclear energy levels [3,7,6,39,40]. Based on the concept of the "equivalent uniform distribution" introduced by Bodmer [43], the nuclear charge distribution is taken as a uniformly charged sphere of radius $R$, where $R$ can be obtained from the experimental value of the root mean square (RMS) nuclear charge radius $\langle R^2\rangle^{1/2}$, as in Eq. (3). For a recent compilation of nuclear charge radii,

see Refs. [44,45]:

$$R = \sqrt{\frac{5}{3}}\langle R^2\rangle^{1/2} \tag{3}$$

The perturbation Hamiltonian (4) is then defined as the difference between the potential of a uniformly charged sphere and the usual Coulomb potential of the point-charge nucleus:

$$\Delta\hat{H} = \begin{cases} -\frac{Z}{2R}\left(3 - \left(\frac{r}{R}\right)^2\right) + \frac{Z}{r}, & r \le R \\ 0, & r > R \end{cases} \tag{4}$$

In Eq. (4), $r$ is the distance from the center of the finite size nucleus. This definition of the perturbation operator implies that the electron density is obtained from the solution of the Schrödinger (or Dirac) equation which employs the point-charge nuclear model. Once the electronic problem is (exactly or approximately) solved, the expectation value of the Hamiltonian (4) yields the energy shift of the nuclear energy level, in the first-order of the perturbation theory.

Within the non-relativistic formalism, it is commonly assumed that the electron density is constant inside the nucleus [6,40]. With this assumption, one obtains Eq. (5) for the expectation value of the operator (4):

$$\Delta E = \frac{2\pi}{5} Z R^2 \bar{\rho}_e \tag{5}$$

where $\bar{\rho}_e$ is the (constant) density inside the nucleus. Adding the energy correction (5) due to the nuclear finite size to the energies of the ground and the excited states of the nucleus and taking into account that the variation of the nuclear radius $\Delta R$ in $\gamma$ transition is small compared to $R$ ($(\Delta R/R) \approx 10^{-4}$) [6,40,41], one obtains Eq. (6) for the $\gamma$ quantum energy shift of the source (absorber) nucleus:

$$\Delta E_\gamma^{a(s)} = \frac{2\pi}{5} Z((R+\Delta R)^2 - R^2)\bar{\rho}_e^{s(a)} \approx \frac{4\pi}{5} Z R^2 \frac{\Delta R}{R}\bar{\rho}_e^{s(a)} \tag{6}$$

Substituting Eq. (6) into Eq. (2), one obtains the usual formula for the Mössbauer isomer shift as a function of the contact density difference between the source and the absorber nuclei [6,7,40]:

$$\delta = \frac{c}{E_\gamma}\frac{4\pi}{5} Z R^2 \left(\frac{\Delta R}{R}\right)(\bar{\rho}_e^a - \bar{\rho}_e^s) \tag{7}$$

Besides the assumption of constant electron density inside the nucleus, the assumption that the fractional variation of the nuclear charge radius, $\Delta R/R$, is independent of the state of the electronic system is implicit in Eq. (7).

### 2.2. Relativistic effects

In theoretical calculations, the contact densities in Eq. (7) are usually represented by the electron density at the nuclear position $\rho(0)$ obtained in the non-relativistic quantum mechanical calculations employing the point-charge nuclear model [6,7,40]. The electronic wave function in the vicinity of nucleus is strongly modified by relativity. For a single electron in the Coulomb field of a point-charge nucleus, the relativistic density near the nucleus behaves as [40,46]:

$$\rho^{rel}(r) = \rho^{nr}(0)\frac{2(1+\sigma)}{\Gamma^2(1+2\sigma)}(2Zr)^{2\sigma-2}, \tag{8}$$

where $\rho^{nr}(0)$ is the non-relativistic density at the nucleus, $Z$ is the nuclear charge and $\sigma = \sqrt{1-\alpha^2 Z^2}$ with the fine structure constant $\alpha$ defined as $\alpha = (e^2/\hbar c) \approx (1/137.035999070(98))$ [47]. The density (8) is divergent near the nucleus, such that the contact density in the relativistic case cannot be defined as $\rho^{rel}(0)$. It should be noted that the density obtained within the scalar-relativistic formalism, that is with neglect of the spin–orbit coupling, is divergent as well due to the divergence in the atomic s wave functions [48].

**Table 1**
Relativistic scaling factors $S'(Z)$ obtained from one-electron atomic model [40] and from many-electron Dirac–Fock calculations [50]

| $Z$ | Ref. [40] | Ref. [50] |
|---|---|---|
| 26 | 1.29 | 1.276 ($Fe^{2+}$–$Fe^{3+}$) [a] |
| 44 | 1.92 | 1.925 ($Ru^{2+}$–$Ru^{3+}$) |
| | | 1.972 ($Ru^{3+}$–$Ru^{4+}$) |
| 77 | 6.21 | 6.225 ($Ir^{2+}$–$Ir^{3+}$) |
| | | 6.941 ($Ir^{3+}$–$Ir^{4+}$) |
| | | 6.719 ($Ir^{4+}$–$Ir^{5+}$) |
| 92 | 12.92 | – |

[a] Based on density difference for the specified charge states of atoms [50].

To bypass the problem of divergent relativistic density at the point nucleus, it was suggested to scale the non-relativistic density at the nucleus $\rho^{nr}(0)$ with an appropriate relativistic scaling factor $S'(Z)$ [40,49–51]. The scaling factors, for a few elements, are shown in Table 1 from which it is obvious that even for elements as light as iron ($Z = 26$) relativity makes a non-negligible contribution to the contact density. The values of the scaling factor $S'(Z)$ have been first analyzed and tabulated by Shirley [40] who employed a one-electron atomic model. In this model, the four-component relativistic $s$ electron density is obtained for a one-electron atom with point-charge nucleus. Then, the expectation value of the perturbation operator (4) is calculated with this density and the scaling factor $S'(Z)$ is obtained by dividing the resulting expression by respective non-relativistic result. The so-obtained relativistic scaling factors were in a fair agreement with the factors $S'(Z)$ obtained later by Mallow et al. [50] from the self-consistent field calculations on many-electron atoms (see Table 1). In the latter calculations, the relativistic electron density obtained in the numeric Dirac–Fock calculations with the point-charge nucleus was averaged over the nuclear volume and compared with the electron density at the nucleus obtained in the numeric Hartree–Fock calculations. In these calculations, it has been noticed that the relativity correction depends on the charge and electronic configuration of the atom (Table 1). Later, Marathe et al. [51] have suggested an interpolation formula $S'(Z) = a + b(n_s - 6) + c(n_d - 6)$ for the scaling factor of iron $^{57}$Fe, which depends on the number of Fe $s$ and $d$ electrons. With this formula, the dependence of the scaling factor $S'(Z)$ on the atomic configuration and charge state is approximately taken into account. This formula was derived from comparison of the orbital contributions $\rho^{MO}(0)$ into the density at the nucleus $\rho(0)$ obtained in the atomic non-relativistic HF calculations with corresponding relativistic values, tabulated by Reschke et al. In this formula, the parameters $a$, $b$, and $c$ depend on the basis set employed in the calculations. With a specific choice of the basis set in Ref. [51], the parameters $a$, $b$, and $c$ take the values of 1.3888898, −0.0000123, and 0.0001636, respectively.

Besides the use of the relativistic scaling factors in combination with the non-relativistic electron densities, the densities calculated within the scalar-relativistic formalism were employed in solid-state band structure calculations in connection with Eq. (7). In these calculations [52–56], the relativistic electron density (obtained in scalar-relativistic formalism with point-charge nucleus) was averaged over a spherical volume with the nuclear charge radius (3). In atomic calculations, a similar approach was used by Mallow et al. [50] to bypass a singularity of the relativistic wave function obtained with the point-charge nucleus.

A direct use of the relativistic or scalar-relativistic densities obtained with the use of the point-charge nucleus should lead to a divergent result for $\rho(0)$, because of the singularity in the atomic

$s$ and $p_{1/2}$ Dirac one-electron wave functions near the nucleus [40,46,50,57]. In the basis set calculations, however, one may not notice these singularities provided that the basis set does not contain extremely tight functions. Seemingly reasonable contact densities can be obtained in this way [58] with the use of common basis sets. These results however should be accepted with a great caution.

The assumption of constant density inside the nucleus is implicit in Eq. (7). This assumption is valid only in the non-relativistic limit [40,57]. For a wave function obtained by a solution of the Dirac equation, the large and the small components are not constant over the nuclear volume. For s electrons in the field of a point-charge nucleus, both components vary in the vicinity of the nucleus as $\psi^L(\mathbf{r})$, $\psi^s(\mathbf{r}) \approx r^{\sigma-1}$, where $\sigma = \sqrt{1-\alpha^2 Z^2}$ and $\alpha$ is the fine structure constant. Integration of the resulting density over the nuclear volume leads to a power dependence of the γ quantum energy shift on the nuclear charge radius [40,59,60]:

$$\Delta E = CR^k \tag{9}$$

which deviates from the quadratic dependence in Eq. (5). In Eq. (9), $C$ is a function of the nuclear charge, of the contact density and of the light velocity. For the exponent $k$, different estimates have been obtained in the literature [40,59,60]. A straightforward application of the first-order perturbation theory with the perturbation Hamiltonian (4) leads to Eq. (10)[40,59]:

$$k = 2\sqrt{1-\alpha^2 Z^2} \tag{10}$$

Dunlap [60] arguing that the solution of the Dirac equation with the point-charge nucleus is singular and is not suitable for the use in perturbational calculations suggested a different formula for the exponential factor $k$:

$$k = 1 + \sqrt{1-\alpha^2 Z^2} \tag{11}$$

It should however be realized that both Eqs. (10) and (11), are based on the consideration of four-component relativistic wave function obtained for hydrogen-like atom. In many-electron atoms, the dependence of the γ quantum energy shift $\Delta E$ on the nuclear charge radius can be slightly different as a consequence of screening of the nuclear charge by other electrons. In any case, Eqs. (10) and (11) show that, for heavy elements, the dependence of $\Delta E$ on $R$ may deviate considerably from the quadratic function and become (nearly) linear for heavy elements [60]. This may require a modification of Eq. (7) for these elements.

### 2.3. Isomer shift as energy derivative

An approach alternative to the use of perturbation theory and Eq. (7) was recently suggested in Ref. [61]. In this approach, a connection between the physical origin of the Mössbauer isomer shift and the origin of the isotope shift of the electronic energy terms was explored [62,63]. The interaction with the nucleus of a finite volume results in the same energy shift of the electronic energy terms as for the nuclear terms. Therefore, assuming that the electronic system remains in the same eigenstate $\Psi_e$ of the electronic Hamiltonian $\hat{H}_e$ during the Mössbauer nuclear transition, the energy shift of the γ quantum can be written as in

$$\Delta E_\gamma = \langle \Psi_e | \hat{H}_e(V_{Ne}^{(e.s.)}) | \Psi_e \rangle - \langle \Psi_e | \hat{H}_e(V_{Ne}^{(g.s.)}) | \Psi_e \rangle \tag{12}$$

where $\hat{H}_e(V_{Ne}^{(g.s.)})$ is the electronic Hamiltonian, which includes the electron–nuclear attraction potential $V_{Ne}^{(g.s.)}$. The latter is the potential of a finite nucleus with the mean square charge radius of the ground state (g.s.) or the excited state (e.s.) of the nucleus. Assuming that the nucleus charge distribution is spherically symmetric and bearing in mind that the variation of the nuclear radius $R$ during the γ transition is extremely small, $(\Delta R/R) \approx 10^{-4}$, one can replace the energy difference in Eq. (12) with the derivatives with respect to the nuclear radius and write Eq. (13) for $\Delta E_\gamma$:

$$\Delta E_\gamma = \left.\frac{\partial E_e(R)}{\partial R}\right|_{R=R_0} \Delta R + \frac{1}{2}\left.\frac{\partial^2 E_e(R)}{\partial R}^2\right|_{R=R_0} (\Delta R)^2 + \cdots \tag{13}$$

In Eq. (13), $E_e(R)$ is the electronic energy calculated with the explicit account of the nucleus of finite size specified by the charge radius $R$ (Eq. (3)), and $R_0$ is the experimentally measured charge radius of the nucleus in the ground state (see, e.g. Ref. [45]). The energy shift of the Mössbauer γ transition is thus defined as a change in the electronic energy due to the variation of the nuclear radius.

With the use of Eq. (13), the Mössbauer isomer shift can be defined as in

$$\delta = \frac{c}{E_\gamma}\left(\left.\frac{\partial E_e^a(R)}{\partial R}\right|_{R=R_0} - \left.\frac{\partial E_e^s(R)}{\partial R}\right|_{R=R_0}\right)\Delta R \tag{14}$$

where only the lowest order derivatives are kept. Eq. (14) implies that the variation of the nuclear radius during the γ transition is independent of the electronic environment and $\Delta R$ remains the same in the source and in the absorber nuclei. In practical calculations with Eq. (14), the electronic energies $E_e^{a(s)}(R)$ can be obtained with the use of a computational scheme which includes the effects of electron correlation and relativity. Therefore, one is not bound to using non-relativistic self-consistent field methods only as it was done within the traditional approach to the isomer shift.

Although the new formula, Eq. (14), appears quite different from the standard perturbational Eq. (7) there is a straightforward connection between the two approaches. Under the assumptions that (i) the electronic energy is obtained variationally (that is, that the Hellmann–Feynman theorem applies), (ii) the nuclear charge distribution is represented by a uniformly charged sphere, and (iii) the electron density inside the nucleus is constant, one obtains Eq. (15) for the derivative of the electronic energy with respect to the nuclear radius [61]:

$$\begin{aligned}\left.\frac{\partial E_e^a(R)}{\partial R}\right|_{R=R_0} &= \left.\left\langle \Psi_e \left| \frac{\partial \hat{H}_e(V_{Ne})}{\partial R} \right| \Psi_e \right\rangle\right|_{R=R_0} \\ &= \left\langle \Psi_e \left| \frac{3Z}{2R_0^4}\sum_i (R_0^2 - r_i^2) H_0(R_0 - r_i) \right| \Psi_e \right\rangle \approx \frac{4\pi}{5} Z R_0 \tilde{\rho}_e\end{aligned} \tag{15}$$

In Eq. (15), index $i$ runs over all the electrons in the system, $r_i$ is the distance between the center of the given nucleus and the $i$th electron, and $H_0(x)$ is the Heaviside step function, which guarantees that the integration in the second line of Eq. (15) is carried out inside a sphere of radius $R_0$ around the nucleus. Substituting (15) in (14) one arrives at Eq. (7). Thus, under the assumptions (i)–(iii), Eq. (14) conforms with the standard perturbational approach to the Mössbauer isomer shift.

It should be realized that the assumptions (i)–(iii) are not implicit in Eq. (14) and that the applicability of the method based on Eqs. (12)–(14) is not restricted to the quantum chemical computational methods based on the variational principle alone, such as the Hartree–Fock method or the Kohn–Sham (KS) density functional theory (DFT) methods. The new approach to the calculation of the isomer shift is based on the reciprocal character of the electron–nuclear interaction and can be applied with any existing quantum chemical method including the methods based on many-body perturbation theory, such as the Møller–Plesset (MP) perturbation theory [64] or coupled cluster (CC) methods [65].

**Table 2**
Theoretical models of nuclear charge distributions employed in quantum chemical calculations (see Ref. [45] for detail)

| Model | Nuclear charge density | Electron–nuclear attraction potential |
|---|---|---|
| Uniformly charged sphere | $\rho_N(R) = \begin{cases} \frac{3Z}{4\pi R_0^3}, & R \le R_0 \\ 0, & R > R_0 \end{cases}$ | $V_{Ne}(r) = \begin{cases} -\frac{Z}{2R_0}\left(3 - \left(\frac{r}{R_0}\right)^2\right), & r \le R_0 \\ -\frac{Z}{r}, & r > R_0 \end{cases}$ |
| Gaussian charge distribution | $\rho_N(R) = \frac{Z}{\pi^{3/2}}\left(\frac{3}{2\langle R^2\rangle}\right)^{3/2} e^{-(3/2)(r^2/\langle R^2\rangle)}$ | $V_N(r) = -\frac{Z}{r}\,\mathrm{erf}\left(\sqrt{\frac{3}{2}\frac{r}{\langle R^2\rangle^{1/2}}}\right)$ |
| Fermi charge distribution | $\rho_N(R) = \frac{\rho_0}{1 + e^{4\ln 3(R-C/T)}}$<br>$\rho_0 = \frac{4\pi}{Z}\int \rho_N(R)R^2\,dR$<br>$C = \sqrt{R_0^2 - \frac{7}{3}\left(\frac{\pi T}{4\ln 3}\right)^2}$<br>$T = 2.30\,\mathrm{fm}$ | No simple analytic formula exists |

Note, that the proper application of the traditional approach based on Eq. (7) in combination with perturbational quantum chemical methods requires the use of the so-called relaxed density matrix (the density matrix which includes the orbital response, Ref. [66]), which is currently not routinely available for the multi-reference extensions of the many-body perturbation theory, such as the complete active space second order perturbation theory (CASPT2) or the multi-reference coupled cluster methods. The use of density matrices without the orbital response leads to incorrect densities [67,68].

In practical application of the approach based on Eq. (14), the derivatives $\partial E_e(R)/\partial R$ are calculated by numeric differentiation of the electronic energy with respect to the nuclear radius [61,69]. In this way, the necessity to compute the relaxed density matrix in MPn or CC calculations is bypassed, which makes the new approach more universal. It has been found in Ref. [61], that the contribution of higher-order terms in the isomer shift is of the order of 0.01% for atomic tin ($Z = 50$). According to Eqs. (9)–(11), the relative contribution of higher-order terms should become even weaker in heavier elements. Therefore, keeping only first derivatives $\partial E_e(R)/\partial R$ in Eq. (14) is a reasonably good approximation.

Formally, Eq. (14) can be brought to the form of Eq. (7) if one defines the effective average electron density inside the nucleus as in

$$\bar{\rho}_e^{a(s)} = \frac{5}{4\pi Z R_0}\left.\frac{\partial E_e^{a(s)}(R)}{\partial R}\right|_{R=R_0} \tag{16}$$

The so-defined effective density $\bar{\rho}_e$ can be used as an analog of the conventional contact density in Eq. (7). The numeric tests carried out in Ref. [61] show that the so-defined density (16) is in a very good agreement with the contact density obtained from the scalar-relativistic wave function by averaging respective density within a sphere of finite radius $R_0$ around the nucleus.

The described approach can be used with any model of nuclear charge distributions, where the most widely used models are summarized in Table 2. In Refs. [61,69], the Gaussian charge distribution (see Table 2) was employed in the numeric calculations. The advantage of this model is that the analytic formulae for the molecular integrals are easily available. It has been argued [61], that the use of different nuclear models should not lead to significant differences in the results as long as the model reproduces the second moment $\langle R^2\rangle$ of the nuclear charge distribution correctly. The difference in the total energies and in orbital energies of atoms obtained with the use of relativistic four-component formalism with all three models listed in Table 2 was studied by Visscher and Dyall [45] and was found to be sufficiently small, $10^{-3}$%, even for an element as heavy as fermium ($Z = 100$).

## 3. Interpretation of Mössbauer isomer shift

From the theoretical interpretation presented in the previous section, the isomer shift δ can be represented as a product of purely atomic quantity (the contact energy difference) and a purely nuclear quantity (the fractional variation of the nuclear charge radius), see Eq. (7). Currently, none of the two quantities can be obtained in the direct experimental measurements [70].

The linear relationship between the contact density and isomer shift is often put in the form:

$$\delta = \alpha\rho(0) + C \tag{17}$$

where $\alpha$ is the calibration constant which absorbs all parameters of the nuclear γ transition in Eq. (7) and $\rho(0)$ is the (relativistically corrected) contact density. Note that the isomer shift is a relative quantity, which is determined for a chemical compound $i$ with respect to another compound $j$, and Eq. (17) can be rewritten as

$$\delta_i - \delta_j = \alpha(\rho_i(0) - \rho_j(0)) \tag{18}$$

in which the additivity constant $C$ is cancelled. Thus, the numeric value of the calibration constant $\alpha$ (cf. Eqs. (7) and (17)) and the fractional nuclear charge radius $\Delta R/R$ (cf. Eqs. (14), (16 and (17)) play crucial role in the interpretation of Mössbauer experiments. Currently, these values cannot be obtained without information on the contact densities calculated with the help of quantum chemical methods.

### 3.1. Nuclear structure parameters

Besides interpretation of Mössbauer experimental data, the calibration constant $\alpha$ provides estimates for the parameters of nuclear structure, specifically for the fractional nuclear charge radius $\Delta R/R$. In a nuclear isomeric pair, the charge (as well as the matter) radius of the ground state is known rather accurately [44]. However, direct experimental information on the radius of the excited states of nuclei (and of the fractional nuclear charge radius $\Delta R/R$) is currently not available.

In principle, the fractional charge radii can be calculated with the use of models of nuclear structure [41]. Theoretical modeling of the nuclear structure within four-component relativistic mean-field theory was quite successfully applied to the calculation of ground state properties, masses and charge radii of various nuclei [71]. However, these models rely primarily on the use of effective nucleon–nucleon interaction potentials which depend on a set of empirical parameters [72,73]. The first principles derivation of these interaction potentials from quantum chromodynamics is

currently not feasible. Thus, in modeling nuclear structure, a complementary information which can be obtained from Mössbauer measurements (and related methods) plays an important role [40–42]. Through the use of Eqs. (7) and (17) in combination with the results of accurate quantum chemical calculations of the contact densities, accurate values of the fractional nuclear charge radii $\Delta R/R$ can be obtained [40,42,49,50,74].

### 3.2. Internal conversion and lifetime measurements

Besides theoretical calculations, complementary information on the contact densities can be obtained in the measurement of the influence of the chemical environment on the internal conversion electron spectra and on the lifetimes of radioactive (isomeric) nuclei [70,75]. In the internal conversion experiments, an electron bound in a specific electronic shell with the binding energy $E_{n'k'}$ is emitted with the kinetic energy of $T_e = E_\gamma - E_{n'k'}$ as a result of internal conversion of the γ quantum with the energy $E_\gamma$. The probability $\alpha_{n'k'}$ of emission from a specific shell is proportional to the electronic density $\rho_{n'k'}(0)$ at the nuclear position for the given shell [70]. Thus, the internal conversion electron spectra give access to the relative contributions of specific electronic shells to the contact density as in

$$\frac{\alpha_{n'_1k'_1}}{\alpha_{n'_2k'_2}} = \frac{\rho_{n'_1k'_1}(0)}{\rho_{n'_2k'_2}(0)} \tag{19}$$

The total contact density influences the lifetime of the isomeric states of nuclei, such that the information on the relative variation of the total contact density $\rho(0)$ with the chemical environment can be accessed through the nuclear excited state lifetime measurements. Measurements of the isomer shift in muonic atoms can also provide an additional set of data on the ratios of the fractional variations in the $\langle R^2\rangle$ (or $\Delta R/R$) in different nuclear γ transitions [75,76]. However, these experiments can only provide an information about the relative variations of contact densities (or partial contact densities $\rho_{n'k'}(0)$) and not about the absolute values of contact densities. Thus, to complete the information necessary for the interpretation of Mössbauer spectra one should rely on the results of quantum chemical calculations of the contact densities.

### 3.3. $^{57}$Fe isomer shift

The best-studied Mössbauer nucleus is $^{57}$Fe, in which the Mössbauer effect is due to the 14.4 keV M1 transition. This nucleus occurred to be extremely difficult for theoretical nuclear structure modeling [40,41]. The first estimate of $-1.8 \times 10^{-3}$ for the fractional charge radius $\Delta R/R$ in $^{57}$Fe isomeric pair was provided by Walker et al. [39] from the interpretation of Mössbauer isomer shifts in a series of iron compounds. The negative value of $\Delta R/R$ implies that the charge radius of the ground state is greater than the radius of the excited state of the nucleus. This unusually large variation in the nuclear charge radius was attributed to zero-point oscillations of the nuclear core [40,41].

Over the years, this value of $\Delta R/R$ was corrected on the basis of new experimental data and theoretical calculations. The accuracy of the calculated contact densities influences strongly the value of the calibration constant $\alpha$ and the estimated fractional radius $\Delta R/R$. From a compilation of the results of early quantum chemical calculations on atomic iron and on iron compounds presented by Duff [74], no convergence to a specific value of $\Delta R/R$ can be seen (see Fig. 1). Fig. 1 presents a compilation of values of the fractional charge radius of $^{57}$Fe nucleus reported by Duff [74] and in later works by other authors. The results of early works on the calibration of $^{57}$Fe

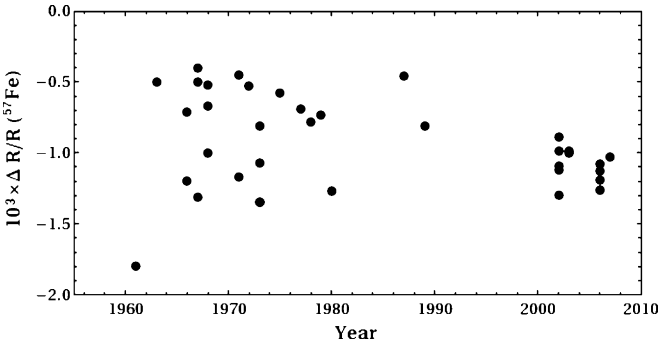


**Fig. 1.** Fractional charge radius $10^3 \times (\Delta R/R)$ of the $^{57}$Fe nucleus as obtained in the past four decades from the interpretation of Mössbauer isomer shift.

isomer shift were analyzed by Oldfield and co-workers [77] who suggested a "consensus" value of $-0.267 \pm 0.115$ for $\alpha(^{57}\text{Fe})$. The large error bars in this value indicate the lack of convergence in the calibration.

The early attempts to interpret the Mössbauer isomer shift were based primarily on the use of densities obtained in the four-component relativistic calculations on bare atoms and cations. In molecular calculations, the atomic densities for the core electrons were combined with the densities obtained for the valence electrons in simplified semi-empirical calculations on iron-containing compounds [78,79]. In these calculations, the contribution of the core electrons was kept frozen and independent on the chemical environment. The so-obtained contact densities showed a reasonably good linear correlation with the isomer shifts for certain compounds however there were spectacular failures in some other cases, such as $BaFeO_4$[78]. Besides that, often the results of calculations on a few molecules only were employed to derive the calibration constant $\alpha$ (and $\Delta R/R$).

Furthermore, the neglect of influence of chemical environment on the core electrons may lead to incorrect results. This was suggested by the experimental measurements on atomic iron embedded in different host metals. From comparison of the results of lifetime measurements of isomeric $^{57}$Fe nuclei in different chemical environments with measurements of the internal conversion probabilities for the same systems, it was found that the variation of contact density is strongly influenced by the inner shells of iron [70]. The discrepancy between the two sets of measurements was sufficiently large: $\Delta\rho(0) = 8.2 \pm 2.2$ bohr$^{-3}$from the lifetime measurements and $1.3 \pm 0.5$ bohr$^{-3}$from the conversion electron spectra [70]. Such a difference could not be explained, if the contribution of the core electrons were constant and independent on the environment. These results clearly demonstrated limitations of the semi-empirical approach adopted for the interpretation of Mössbauer measurements [78].

Later, all-electron *ab initio* self-consistent field calculations on molecular models of solids and on matrix-isolated molecules were started [30,31,51,80] with the purpose of interpretation of Mössbauer isomer shifts. These calculations relied primarily on the non-relativistic self-consistent field formalism. The effect of relativity has been introduced through the use of relativistic scaling factors $S'(Z)$ in Eq. (7). Most often, this factor was assumed independent on the electronic configuration of the atom. However, it has been noticed that the ratio of relativistic and non-relativistic contact densities depends on the electronic configuration [50] and a simple empirical formula relating $S'(Z)$ with the orbital populations was suggested [51].

The effect of electron correlation on the contact densities in a series of matrix-isolated iron-containing molecules was studied in Refs. [30,31,51]. In these works, Møller–Plesset many-body per-

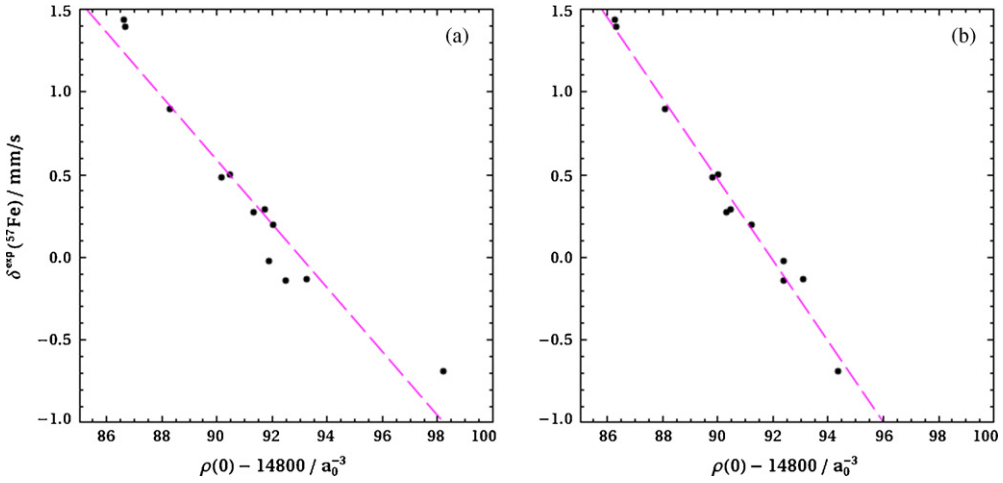


**Fig. 2.** Calculated electron contact density compared to experimental isomer shifts for iron clusters and molecules. Panel (a) shows the density obtained with relativistically corrected HF method. The densities obtained with relativistically corrected MP2 method are shown in panel (b). Cited from Refs. [61,69].

turbation theory up to fourth order was used. It was found that, in spite of a decisive effect of electron correlation on the relative energies of the studied molecules, the effect of electron correlation on the calculated contact densities was rather weak. Note however that, in these works, the total densities were obtained without inclusion of the orbital relaxation, which is important for obtaining accurate density matrices in the computational methods violating Hellmann–Feynman theorem [66–68].

Recently [61,69], the effect of electron correlation on the calculated Mössbauer isomer shift in a series of iron compounds was studied with the help of a new approach described in Section 2.3. Within this approach, the isomer shift (and the contact density) is obtained by differentiation of the total electronic energy with respect to the radius of finite nucleus as in Eqs. (14) and (16). Thus, the necessity to compute relaxed density matrix in connection with advanced quantum chemical methods is avoided. Although a parametrization of the calibration constant $\alpha$ was not attempted in Refs. [61,69], the available information enables one to parametrize $\alpha$ (and $\Delta R/R$) for $^{57}$Fe. In Fig. 2, the results of relativistically corrected (with the scalar-relativistic effects included) Hartree–Fock and MP2 calculations [61,69] on a set of iron-containing clusters and molecules standardly used [77,80–82] for the parametrization of $^{57}$Fe isomer shift are presented. Linear regression analysis shows clearly that the inclusion of electron correlation has a noticeable effect on the calibration constant, $\alpha_{HF}(^{57}Fe) = -0.193 \pm 0.017 a_0^3$ mm s$^{-1}$ and $\alpha_{MP2}(^{57}Fe) = -0.244 \pm 0.009 a_0^3$ mm s$^{-1}$, and the quality of correlation between the calculated contact density and the experimental isomer shift, $r^2_{HF} = 0.929$ vs. $r^2_{MP2} = 0.984$. These values of $\alpha(^{57}Fe)$ are in agreement with the calibration constants obtained in earlier works by Trautwein et al. ($-0.249 \pm 0.025$) [79] and Nieuwpoort et al. ($-0.22 \pm 0.02$) [80]. It has also been observed in the HF, MP2, and CCSD(T) calculations on a set of coinage metal atoms [61] that the electron correlation has a strong effect (up to 50%) on the density differences between different states of atoms. Thus, the use of a universal value for the relativistic scaling factor $S'(Z)$ may lead to inaccurate results.

Density functional theory furnishes another approach to include the effect of electron correlation in quantum chemical calculations. Density functional methods are known to include correlation effects by construction, albeit in an approximate and model way. There exists a large variety of approximate density functionals which enable one to obtain results of acceptable accuracy for geometry and thermochemistry of large molecules. Although the methods related to density functional theory, such as the Xα method [83], were employed for the interpretation of Mössbauer spectra for a long time [84–89], the use of more accurate density functional approaches in these calculations was initiated relatively recently [56,58,77,81,82,90–92].

Density functional calculations of molecular models of solids [58,77,81,82,90–92] as well as band structure calculations [55,56] have been employed to obtain the contact densities in iron compounds. Large sets of iron-containing species have been used in the calculations to reduce the dependence of the calibration constant on the choice of the training set of compounds. However, in spite of the calibration on large sets of compounds, these calculations were not capable to deliver a converged value for the calibration constant $\alpha$. The numeric value of $\alpha$ (and of $\Delta R/R$) shows strong dependence on the choice of the particular density functional and the basis set employed in the calculations and can vary by as much as 20–30%. Thus, the values in the range $-0.253$ to $-0.367 a_0^3$ mm s$^{-1}$ were obtained by different authors for the calibration constant $\alpha$ of $^{57}$Fe, which leads to the values of $\Delta R/R$ varying in the range $-0.89 \times 10^{-3}$ to $-1.30 \times 10^{-3}$ [56,77,81,82]. It should be noticed however that modern density functionals do not correctly describe the electron–electron interaction potential in the vicinity of nucleus. The potential generated by the gradient corrected density functionals is divergent near the point-charge nucleus [93], which may lead to deterioration of the contact densities obtained with these functionals [69].

### 3.4. Isomer shift of $^{119}$Sn and other Mössbauer nuclei

Besides $^{57}$Fe the fractional charge radii have been determined for a number of other Mössbauer nuclei. One of the most well investigated cases is the $^{119}$Sn nucleus. Nuclear structure models yielded, for the 23.87 keV M1 transition in $^{119}$Sn nucleus, a value of the fractional charge radius varying between $1.1 \times 10^{-4}$ [94] and $0.76 \times 10^{-4}$. [41] Initially, there was a disagreement on the sign of $\Delta R/R$ with some works predicting negative value for $\Delta R/R$ ($-2.5 \times 10^{-4}$) [95]. This controversy was later resolved in favor of the positive value of the fractional charge radius [4].

Similarly to $^{57}$Fe, there is a large spread in the values of the fractional charge radius determined for $^{119}$Sn with the use of different methods. As shown in Fig. 3, the values of $\Delta R/R$ of $^{119}$Sn range between a value of $3.3 \times 10^{-4}$ [96] obtained from internal con-

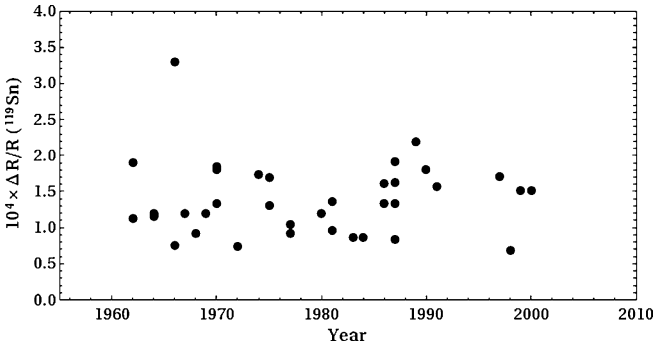


**Fig. 3.** Fractional charge radius $10^4 \times (\Delta R/R)$ of the $^{119}$Sn nucleus as obtained in the past four decades from the interpretation of Mössbauer isomer shift.

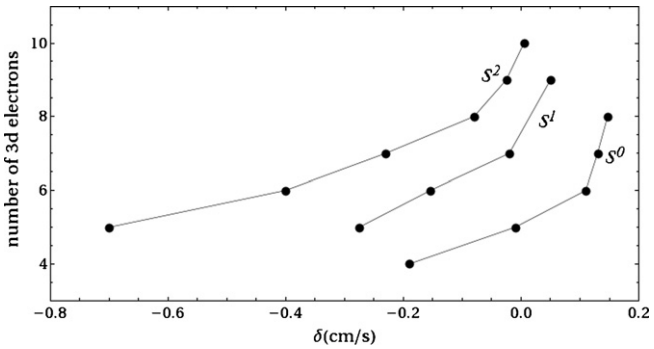


**Fig. 4.** Relation between isomer shift and the number of 3d electrons for different number of 4s electrons in $^{57}$Fe. Reproduced from Ref. [113].

version electron spectra and a value of $0.69 \times 10^{-4}$ [97] obtained from interpretation of the electron capture experiments on $^{113}$Sn nucleus.

Quantum chemical calculations undertaken on tin compounds led to values of $\Delta R/R$ clustering around $1.8 \times 10^{-4}$. Typically, scalar-relativistic quantum chemical formalism was employed for the interpretation of $^{119}$Sn Mössbauer data. In these calculations, the contact density was obtained from averaging of the scalar-relativistic total density obtained in solid-state Xα or DFT calculations inside a sphere of nuclear charge radius [52,53,98–104]. Similarly to the case of $^{57}$Fe, majority of these calculations have been carried out for a few compounds of the target element. Later, in works by Svane et al. [53] and Lippens [105] a parametrization of the fractional charge radius of $^{119}$Sn against an extended set of tin compounds was undertaken. A value of $(1.72 \pm 0.04) \times 10^{-4}$ was obtained in Ref. [53] for $\Delta R/R$ of $^{119}$Sn. This value is consistent with the estimates obtained from the analysis of Mössbauer data in Refs. [105,106].

Calibration constants $\alpha$ and fractional charge radii $\Delta R/R$ for several Mössbauer nuclei are collected in Table 3[107–112]. In determination of these parameters, the results of quantum chemical calculations of the contact densities $\rho(0)$ or partial contact densities $\rho_{n'k'}(0)$ have been used in the interpretation of Mössbauer and internal conversion experiments. It should be realized that the accuracy of these data relies critically on the accuracy of the quantum chemical calculations. In view of considerable improvement in the predictive power of quantum chemical methods, the constants reported in Table 3 and the data reported in Ref. [6] may need a substantial update.

## 4. Theoretical modeling of isomer shift

After the first observation of the isomer shift in α-$Fe_2O_3$ by Kistner and Sunyar [37], it soon became apparent that the isomer shift δ provides information on the electronic configuration of the resonating atom and its chemical environment. Theoretical models relate the changes in δ with the electron density at the nucleus [38,39], which is influenced by the factors such as the oxidation and spin state of the Mössbauer atom, covalent bonding to the surrounding atoms (ligands), and the geometry of the coordination sphere of the resonating atom.

### 4.1. Free atomic ion models

The first theoretical interpretation of the $^{57}$Fe isomer shift by Walker et al. [39] related variations in the contact density $\rho(0)$ to the populations of the atomic d and s orbitals in the given oxidation state of iron. Because high-level all-electron quantum chemical calculations on molecules were not yet available, the results of atomic calculations on a number of oxidation states of iron were used to explain the variations in the $^{57}$Fe isomer shift. Later, this relationship was extended by Brady et al. [113] by adding some extrapolated theoretical and experimental data. A diagram, which related the $^{57}$Fe isomer shift with the number of atomic s and d electrons was devised [113]. In Fig. 4, the so-obtained relationship between isomer shift and the number of 3d electrons in $^{57}$Fe atomic species is reproduced from Ref. [113].

The variations of the contact density in $^{57}$Fe have been initially interpreted as dominated by the contribution of atomic 3s electrons, which is influenced by the screening due to 3d electrons.

**Table 3**
Fractional charge radius $\Delta R/R$ and isomer shift calibration constant $\alpha$ of several Mössbauer nuclei

| Isotope | Isomeric transition (keV) | $\Delta R/R$ | $\alpha$ ($a_0^3$ mm s$^{-1}$) | Ref. |
|---|---|---|---|---|
| $^{57}$Fe | 14.4 | $(-0.82 \pm 0.07) \times 10^{-3}$ | $-0.23 \pm 0.02$ | [74] |
| | | $(-0.885 \pm 0.090) \times 10^{-3}$ | $-0.249 \pm 0.025$ | [79] |
| | | $(-0.78 \pm 0.07) \times 10^{-3}$ | $-0.22 \pm 0.02$ | [80] |
| | | $(-0.948 \pm 0.408) \times 10^{-3}$ | $-0.267 \pm 0.115$ | [77] |
| $^{61}$Ni | 67.4 | $(-0.27 \pm 0.13) \times 10^{-4}$ | $(-1.8 \pm 0.9) \times 10^{-3}$ | [107] |
| $^{67}$Zn | 93.3 | $(7.0 \pm 1.0) \times 10^{-4}$ | $0.039 \pm 0.006$ | [100] |
| $^{119}$Sn | 23.8 | $(1.72 \pm 0.04) \times 10^{-4}$ | $0.092 \pm 0.002$ | [53] |
| $^{121}$Sb | 37.15 | $(-10.4 \pm 1.0) \times 10^{-4}$ | $-0.368 \pm 0.035$ | [100] |
| | | $-12.36 \times 10^{-4}$ | $-0.4376$ | [131] |
| $^{125}$Te | 35.46 | $(0.853 \pm 0.115) \times 10^{-4}$ | $0.033 \pm 0.004$ | [108] |
| | | $0.8 \times 10^{-4}$ | 0.031 | [109] |
| $^{127}$I | 57.6 | $-3.4 \times 10^{-4}$ | $-0.083$ | [109] |
| $^{129}$I | 27.8 | $4.3 \times 10^{-4}$ | 0.221 | [109] |
| | | $4.18 \times 10^{-4}$ | 0.215 | [120] |
| | | $4.1 \pm 0.1 \times 10^{-4}$ | $0.211 \pm 0.005$ | [110,111] |
| $^{197}$Au | 77.3 | $1.4 \pm 0.3 \times 10^{-4}$ | $0.051 \pm 0.011$ | [112] |

Thus, removal of a 3d electron should lead to a weaker screening and to an increase of the contact density. The contact density increases also upon addition of a 4s electron [39,113]. Because of the negative fractional charge radius $\Delta R/R$ of $^{57}$Fe, the increase in the contact density results in a negative isomer shift. In this way, an interpolation formula for the isomer shift δ as a function of the (fractional) occupation numbers of the atomic valence orbitals was designed and parametrized on the basis of comparison with the experimental data [114,115].

### 4.2. Molecular and cluster models

The first molecular calculations of the isomer shift were carried out by Trautwein and co-workers [78,79,116–120]. Because of computational restrictions, these calculations employed an iterative Hückel method combined with a semi-empirical configuration interaction treatment of the open-shell species. Within such an approach, the contributions of the inner atomic orbitals into the contact density $\rho(0)$ could not be directly obtained and one had to resort to the use of the densities of the core s orbitals at the nucleus obtained in the atomic self-consistent field calculations. For the sub-valence (3s, in the case of iron) orbitals, the orthogonality corrections of the type suggested in Ref. [121] were employed. The contributions of deeper core s orbitals were kept constant. This procedure, however, was criticized by Duff [74] for neglecting the important orthogonality corrections with the deeper core orbitals, 2s–3s orthogonality in the case of iron.

Duff was probably the first to carry out an all-electron molecular self-consistent field calculation of the contact density for the interpretation of isomer shift [74]. The first computational work on the cluster $FeF_6^{3-}$ [74] was soon followed by the work of Nieuwpoort et al. [80] who studied a series of small cluster models of iron compounds and found a good linear correlation between the theoretical contact densities and the experimental isomer shifts. Although, in these calculations, a number of negatively charged clusters with the total charge up to -4 were considered, the effect of the crystalline environment on the calculated contact densities was found to be negligibly small [80]. The all-electron *ab initio* calculations were found to yield results closer to experimental data than the semi-empirical methods based on the iterative Hückel theory or the self-consistent charges Xα (SCC-Xα) method [122].

Early calculations of isomer shift were based on the use of the contact densities obtained in self-consistent calculations, which neglect effect of the electron correlation. Calculations of the contact densities in small iron molecules, which included the electron correlation via the use of Møller–Plesset many-body perturbation theory up to the fourth order, were undertaken in Refs. [30,31,51] with the purpose of interpretation of Mössbauer measurements on matrix-isolated iron compounds. In these calculations, it has been found that the effect of electron correlation on the contact densities is insignificant. However, the orbital response contribution into the density matrix was not taken into account in these calculations. This contribution is important for obtaining the correct density matrix and the first-order response properties in quantum chemical methods based on many-body perturbation theory or in truncated configuration interaction methods [66–68]. Later, in a set of calculations on a series of iron-containing complexes and various charge and spin states of coinage metal atoms carried out in Ref. [61] with the use of the method described in Section 2.3, it was found that the electron correlation makes a non-negligible contribution into the contact densities and isomer shifts. The results obtained in Ref. [61] with the use of the MP2 method show considerably better correlation with the experimental isomer shifts than the Hartree–Fock results (see Fig. 2).

### 4.3. Density functional and ab initio calculations

The use of modern methods based on density functional theory (DFT) for the investigation of Mössbauer isomer shift was initiated relatively recently. It should be noted that density functional theory in the form of Xα method, which has been suggested by Slater et al. [83] as an approximation to the Hartree–Fock method, has been applied by several authors to the investigation of Mössbauer parameters already in 1970s [84–86,103,104]. More accurate density functional methods were first used in the works of Oldfield and co-workers [77] and Noodelman and co-workers [91,92] who applied these methods to the investigation of Mössbauer parameters of organometallic and bio-organic iron compounds. These initial calculations have demonstrated utility of density functional methods for understanding of relationships between the electronic structure of complex biological molecules and the observed parameters of Mössbauer spectra. These initial applications of DFT methods have been extended in the works of Neese and co-workers [58,81,90] and Nemykin and co-workers [82].

An analysis of the results of density functional calculations of the isomer shift shows [81] that the traditional interpretation of the trends in terms of the orbital populations is not completely reliable. In the traditional interpretations it is assumed: (i) that the variations in the 3s shell of iron dominate the variations in the contact density and the isomer shift; (ii) that the 3d orbitals influence the isomer shift via screening of the 3s and 4s electrons; and (iii) that the 4s shell influences the isomer shift via its population. In contrast with these assumptions, it has been found by Neese [81]: (a) that the $^{57}$Fe isomer shift is largely (up to 70%) dominated by the contributions from valence orbitals (that is 4s and 3d orbitals) and the contribution of the 3s shell is relatively minor; (b) that the population of the 4s orbital of iron does not correlate with the trend in the contact density and isomer shift; and (c) that the valence contribution to the isomer shift is influenced by covalency effects, molecular geometry and the screening due to 3d electrons which alters the shape of the 4s shell. It was emphasized that the actual populations of the iron 3d orbitals are quite different from the formal valencies of iron atoms in compounds. Therefore, simple arguments based on the crystal field picture should be accepted with caution [81].

A similar conclusion about the role of covalency effects and molecular geometry for the $^{57}$Fe isomer shift has been recently reached on the basis of the complete active space self-consistent field (CASSCF) investigation of the isomer shift in a series of iron complexes [123]. Analysis of the CASSCF wave functions carried out in terms of localized orbitals demonstrated that the greatest differential effect on the isomer shift originates from the contribution of the tails of the ligand-dominated orbitals. A linear correlation between the isomer shift and the difference between the formal oxidation degree of iron atom and its actual computed charge was observed. Such a correlation suggests a relationship between the isomer shift and the Fe–ligand bond covalency [123] thus supporting the conclusions reached on the basis of density functional calculations [81].

In density functional studies, it has been observed that the calibration constant $\alpha$, in Eqs. (7), (17), and (19), depends of the choice of the atomic orbital basis set and on the choice of density functional employed [58,77,81,82,90–92,124–130]. It has been suggested that, for every combination of basis set and approximate density functional, an individual value of the calibration constant should be obtained [81,82]. Such a semi-empirical approach, however successful can it be, does not allow for a determination of the nuclear γ transition parameters from first principles [81].

In Ref. [69], the question of applicability of density functional theory methods for the interpretation of the isomer shift was

addressed with the help of the approach described in Section 2.3. It has been found that with the use of a single calibration constant $\alpha$, which has been adopted from the Ref. [6], the isomer shifts calculated with a variety of methods ranging from *ab initio* HF and MP2 methods to hybrid HF/DFT density functionals show reasonably good correlation with the experimental values [69]. The correlation with the experiment improves with the increase in the basis set size and with the inclusion of electron correlation in *ab initio* methods. The best results have been produced by the hybrid HF/DFT density functionals with relatively large fraction of the HF exchange, such as the BH&HLYP functional. Relatively poor performance of pure density functionals, such as BLYP, was explained as originating from the divergence of the Kohn–Sham potential generated by these functionals near the nucleus [93]. Thus, a single calibration constant $\alpha$ can be employed in theoretical modeling of isomer shift for the given element, the value of which can be obtained in the high-level *ab initio* calculations with inclusion of the electron correlation.

### 4.4. Inclusion of relativistic effects

In the calculations on iron (as well as on some other elements), the non-relativistic quantum chemical formalism is usually employed in connection with the cluster approach [77,80–82,85,86,88,89,103,104,124–130]. The so-obtained contact densities are corrected for relativistic effects with the use of scaling factor $S'(Z)$. It has been argued that the use of this factor in the calibration procedure is unimportant [81], because $S'(Z)$ has the same value for all compounds of the given element. It should be realized however, that the universality of the scaling factor for a given element was postulated in early works on the isomer shift [40]. Later, it has been found that the relativistic scaling factor is different for different charge and spin states of the same atom [50] and an empirical formula relating $S'(Z)$ to the occupation numbers of the atomic orbitals was suggested [51].

Direct inclusion of relativistic effects in molecular calculations has been attempted in Refs. [58,61], and [69] and quite different conclusions have been drawn in these works. In Ref. [58], it has been argued that the inclusion of relativistic effects did not bring a noticeable improvement and that the contact densities can be calculated within the non-relativistic formalism. It should be noted that the contact densities in Ref. [58] were obtained as the density at the nuclear position $\rho(0)$, which in case of relativistic formalism should lead to a divergent result [40,46]. This divergence may not be noticed in the calculations which employ standard basis sets composed of functions regular at the nuclear position. However, physical meaning of the so-obtained results can be questioned. A different conclusion on the role of relativistic effects was reached in Refs. [61] and [69] where the approach described in Section 2.3 was employed. On the basis of comparison between the relativistic and the non-relativistic isomer shifts obtained with the use of the same formalism, it was found that inclusion of relativity is important for obtaining accurate results from molecular (cluster) models. It is noteworthy that scalar-relativistic solid-state calculations are routinely carried out in the study of Mössbauer parameters of crystalline solids [53,55,56,87,100–102,105,106,131].

### 4.5. Solid-state calculations of isomer shift

The inclusion of solid-state effects into the $^{57}$Fe isomer shift calculation was undertaken in Refs. [55,56,87]. In these works, the scalar-relativistic solid-state calculations on a number of crystalline iron compounds have been carried out. The contact densities were obtained by averaging of the calculated density inside a sphere of the nuclear charge radius. Although very similar computational approaches were used in both works, two quite different values for the calibration constant $\alpha(^{57}\mathrm{Fe})$ were obtained: a value of $-0.22a_0^3$ mm s$^{-1}$was obtained in Ref. [87] and a value of $-0.291a_0^3$ mm s$^{-1}$ was reported in Ref. [56]. This difference can most likely be attributed to the use of different density functional methods in the two works and to the use of small sets of compounds for the calibration. Interesting to note, that the value $\alpha = -0.291a_0^3$ mm s$^{-1}$obtained by Wdowik and Ruebenbauer [56] is fairly close to the values obtained by Oldfield et al. [77] in density functional calculations on cluster models of solids. Therefore, the role of solid-state effects for calibration of the isomer shifts is, probably, not very significant.

Computational modeling of the isomer shift for other nuclei has evolved in time along similar route as for $^{57}$Fe. Thus, early attempts concentrated on the calculations for free ions carried out at the level of the Hartree–Fock (or Dirac–Fock) method or of the Xα method. An overview of the early works on the Mössbauer spectroscopy of $^{119}$Sn, $^{121}$Sb, $^{125}$Te, $^{127,129}$I, $^{129}$Xe, and some rare earth elements, such as $^{151}$Eu, can be found in Ref. [132]. These early works resulted in a number of empirical relationships between the occupation numbers of the valence orbitals of resonating atom and its isomer shift. At a later stage, calculations on cluster models [103,104,133–138] as well as solid-state calculations [53,100–102,105,106,131] have been carried out.

For $^{119}$Sn nucleus, recent calculations of Svane et al. [53] which have been carried out with the inclusion of scalar-relativistic and solid-state effects on a broad range of tin crystalline compounds have produced a value of $0.092 \pm 0.002$ for the calibration constant $\alpha$. This value is in a reasonable agreement with $\alpha = 0.084 \pm 0.007$ obtained by Guenzburger and co-workers in cluster calculations [88,89,104]. The proximity of the results of two different sets of calculations (solid state and cluster) indicates that the role of solid-state effects can be not very significant and that one can safely use reasonable cluster models of solids. Such a conclusion is in agreement with the observations about minor importance of crystalline environment for the isomer shift made on the basis of quantum chemical calculations [80] and experimental observations on matrix-isolated molecules. In the latter case, it has been observed experimentally that the isomer shifts in matrix-isolated molecules $TeF_6$ and $TeCl_4$ are nearly identical to the shifts of the respective condensed compounds [132].

Although accurate calculations of tin calibration constant carried out at the solid-state level and at the molecular level have reached a reasonable degree of convergence, the question of the precise numeric value of $\alpha(^{119}\mathrm{Sn})$ does not seem to be completely settled. In a set of calculations, carried out in Ref. [138] on a number of cluster models of tin chalcogenides a quite different value for the calibration constant $\alpha = 0.112$ [139] has been obtained. The latter calculations have been carried out at the non-relativistic level with the use of local density approximation within DFT. The difference in the parametrized values of the calibration constant underlines the necessity to carry out the isomer shift calibration on a representative set of compounds of a given element and with the use of high-level *ab initio* calculations with the inclusion of both relativistic and electron correlation effects.

## 5. Perspective

An important feature of Mössbauer spectroscopy and related methods, such as time-differential perturbed angular correlation spectroscopy [24] and methods based on scattering of synchrotron radiation [17–23], is that these methods provide information about the electronic structure of materials on an atomic scale. Information on the local chemical environment of the resonating nucleus is provided by the isomer shift of a nuclear transition energy. This parameter is influenced by the oxidation and spin state of the

resonating atom, by covalency effects and geometry of the local coordination sphere [3,5–7].

Further advancement of the Mössbauer techniques requires that the following important aspects have to be addressed: (i) First, the nuclear structure parameters, such as the fractional charge radii $\Delta R/R$, which determine the relationship between the observed isomer shift and the electron contact density (see Eqs. (7), (17) and (18)), need to be accurately determined to allow a reliable determination of the electronic structure parameters from the measured velocities. (ii) The interpretation of the observed trends in the isomer shift requires gaining knowledge on the ways in which the local chemical environment influences the parameters of Mössbauer spectra. Addressing these points is impossible without accurate theoretical calculations of Mössbauer parameters.

The latter task is especially challenging for the quantum chemical methods, because it requires the inclusion of effects such as relativity and electron correlation. *Ab initio* calculations over a wide range of chemical environments have to be carried out for reliable calibration of Mössbauer spectroscopy parameters and determination of universal, method-independent constants [53]. In this respect, development of the first principles approaches, which go beyond the traditional perturbational treatment of isomer shift and incorporate inherently the aforementioned effects of relativity and electron correlation, should lead to a substantial progress towards a more accurate theoretical interpretation of Mössbauer spectra. In combination with the high-level computational approaches to the calculation of other nuclear parameters, such as quadrupole splitting [140–149] and hyperfine splitting constants [150–152], these developments will ultimately lead to a full theoretical characterization of Mössbauer spectra and to deeper understanding of their relationship with the electronic structure of materials.

## References


[1] R.L. Mössbauer, Z. Phys. 151 (1958) 124.
[2] A.J.F. Boyle, H.E. Hall, Rep. Prog. Phys. 25 (1962) 441.
[3] G.K. Wertheim, Mössbauer Effect: Principles and Applications, Academic Press, New York, 1964.
[4] V.I. Gol'danski, Sov. Phys. Usp. 9 (1967) 461.
[5] P. Gütlich, in: U. Gonzer (Ed.), Mösbauer Spectroscopy, Springer, Berlin, 1975, p. 53.
[6] G.K. Shenoy, F.E. Wagner (Eds.), Mössbauer Isomer Shifts, North-Holland, Amsterdam, 1978.
[7] P. Gütlich, R. Link, A. Trautwein, Mössbauer Spectroscopy and Transition Metal Chemistry, Springer, Heidelberg, 1978.
[8] Yu.M. Kagan, I.S. Lyubutin (Eds.), Applications of the Mössbauer Effect, vol. 4. Materials Science, Gordon and Breach, New York, 1985.
[9] P. Gütlich, J. Ensling, in: E.I. Solomon, A.B.P. Lever (Eds.), Inorganic Electronic Structure and Spectroscopy, vol. I, Wiley, New York, 1999, p. 161.
[10] M.D. Dyar, D.G. Argesti, M.W. Schaefer, C.A. Grant, E. Sklute, Annu. Rev. Earth Planet. Sci. 34 (2006) 83.
[11] E. Münck, in: L. Que Jr. (Ed.), Physical Methods in Bioinorganic Chemistry: Spectroscopy and Magnetism, University Science Books, Sausalito, 2000, p. 287.
[12] E. Münck, A. Stubna, in: J.A. McCleverty, T.B. Meyer, A.B.P. Lever (Eds.), Comprehensive Coordination Chemistry II, vol. 2. Fundamentals: Physical Methods, Theoretical Analysis and Case Studies, Elsevier, New York, 2003, p. 279.
[13] S. Mørup, Mössbauer Effect Ref. Data J. 25 (2002) 105.
[14] S.J. Campbell, W.A. Kaczmarek, M. Hofmann, Hyperfine Interact. 126 (2000) 175.
[15] S.D. Forder, AIP Conf. Proc. 765 (2005) 307.
[16] G. Klingelhöfer, et al., Science 306 (2004) 1740, and reference cited therein.
[17] O. Leupold, J. Pollmann, E. Gerdau, H.D. Rüter, G. Faigel, M. Tegze, G. Bortel, R. Rüffer, A.I. Chumakov, A.Q.R. Baron, Europhys. Lett. 35 (1996) 671.
[18] I. Koyama, Y. Yoda, X.W. Zhang, M. Ando, S. Kikuta, Jpn. J. Appl. Phys. 35 (1996) 6297.
[19] R. Coussement, S. Cottenier, C. L'abbé, Phys. Rev. B 54 (1996) 16003.
[20] G. Neyens, J. Odeurs, R. Coussement, C. L'abbé, S. Cottenier, J. Ladrière, Hyperfine Interact. 111 (1998) 341.
[21] O. Leupold, A.I. Chumakov, E.E. Alp, W. Sturhahn, A.Q.R. Baron, Hyperfine Interact. 123–124 (1999) 611.
[22] C. L'abbé, R. Callens, J. Odeurs, Hyperfine Interact. 135 (2001) 275.
[23] A. Konjhodzic, A. Adamczyk, F. Vagizov, Z. Hasan, E.E. Alp, W. Sturhahn, J. Zhao, J.J. Carroll, Hyperfine Interact. 170 (2006) 83.
[24] D.A. Shirley, H. Haas, Annu. Rev. Phys. Chem. 23 (1972) 385.
[25] T.K. McNab, H. Micklitz, P.H. Barrett, Phys. Rev. B 4 (1971) 3787.
[26] F.J. Litterst, A. Schichl, E. Baggiosaitovitch, H. Micklitz, J.M. Friedt, Ber. Bunsen.-Phys. Chem. Chem. Phys. 82 (1978) 73.
[27] M. Braga, A.R. Riego, J. Danon, Phys. Rev. B 22 (1979) 5128.
[28] C.H.F. Peden, S.F. Parker, P.H. Barrett, R.G. Pearson, J. Phys. Chem. 87 (1983) 2329.
[29] M. Pasternak, Hyperfine Interact. 27 (1986) 173.
[30] E.L. Bominaar, J. Guilin, V.R. Marathe, A. Sawaryn, A.X. Trautwein, Hyperfine Interact. 40 (1988) 111.
[31] E.L. Bominaar, J. Guilin, A. Sawaryn, A.X. Trautwein, Phys. Rev. B 39 (1989) 72.
[32] Y. Einaga, Y. Yamada, T. Tominaga, J. Radioanal. Nucl. Chem. 218 (1997) 97.
[33] Y. Yamada, Hyperfine Interact. 139 (2002) 77.
[34] R.L. Cohen, Science 178 (1972) 828.
[35] P. Boolchand, P. Boolchand (Eds.), Insulating and Semiconducting Glasses. Series on Directions in Condensed Matter Physics, vol. 17, World Scientific, Singapore, 2000, p. 191.
[36] J.M. Grenèche, J. Non-Cryst. Sol. 287 (2001) 37.
[37] O.C. Kistner, A.W. Sunyar, Phys. Rev. Lett. 4 (1960) 412.
[38] S. DeBenedetti, G. Lang, R. Ingalls, Phys. Rev. Lett. 6 (1961) 60.
[39] L.R. Walker, G.K. Wertheim, V. Jaccarino, Phys. Rev. Lett. 6 (1961) 98.
[40] D.A. Shirley, Rev. Mod. Phys. 36 (1964) 339.
[41] R.A. Uher, R.A. Sorensen, Nucl. Phys. 86 (1966) 1.
[42] J. Speth, W. Henning, P. Kienle, J. Meyer, in: G.K. Shenoy, F.E. Wagner (Eds.), Mössbauer Isomer Shifts, North-Holland, Amsterdam, 1978, Chapter 13.
[43] A.R. Bodmer, Proc. Phys. Soc., London, Sect. A 66 (1953) 1041.
[44] G. Fricke, C. Bernhardt, K. Heilig, L.A. Schaller, L. Schellenberg, E.B. Shera, C.W. de Jager, At. Data Nucl. Data Tables 60 (1995) 177.
[45] L. Visscher, K.G. Dyall, At. Data Nucl. Data Tables 67 (1997) 207.
[46] G. Breit, Phys. Rev. 42 (1932) 348.
[47] G. Gabrielse, D. Hanneke, T. Kinoshita, M. Nio, B. Odom, Phys. Rev. Lett. 97 (2006) 030802;
G. Gabrielse, D. Hanneke, T. Kinoshita, M. Nio, B. Odom, Phys. Rev. Lett. 99 (2007) 039902.
[48] S. Blügel, H. Akai, R. Zeller, P.H. Dederichs, Phys. Rev. B 35 (1987) 3271.
[49] J.L.K.F. de Vries, J.M. Trooster, P. Ros, J. Chem. Phys. 63 (1975) 5256.
[50] J.V. Mallow, A.J. Freeman, J.P. Desclaux, Phys. Rev. B 13 (1976) 1884.
[51] V.R. Marathe, A. Sawaryn, A.X. Trautwein, M. Dolg, G. Igel-Mann, H. Stoll, Hyperfine Interact. 36 (1987) 39.
[52] E. Antoncik, Phys. Stat. Sol. (b) 79 (1977) 605.
[53] A. Svane, N.E. Christensen, C.O. Rodriguez, M. Methfessel, Phys. Rev. B 55 (1997) 12572.
[54] P. Mohn, Hyperfine Interact. 128 (2000) 67.
[55] A. Falepin, S. Cottenier, C.M. Comrie, A. Vantomme, Phys. Rev. B 74 (2006) 184108.
[56] U.D. Wdowik, K. Ruebenbauer, Phys. Rev. B 76 (2007) 155118.
[57] B.D. Dunlap, G.M. Kalvius, Mössbauer Isomer Shifts (Ref. [6]), Chapter 2.
[58] S. Sinneker, L.D. Slep, E. Bill, F. Neese, Inorg. Chem. 44 (2005) 2245.
[59] G. Breit, Rev. Mod. Phys. 30 (1958) 507.
[60] B.D. Dunlap, Phys. Rev. A 6 (1972) 2057.
[61] M. Filatov, J. Chem. Phys. 127 (2007) 084101.
[62] D.N. Stacey, Rep. Prog. Phys. 29 (1966) 171.
[63] R. Weiner, Phys. Rev. 114 (1959) 256.
[64] C. Møller, M.S. Plesset, Phys. Rev. 46 (1934) 618;
for a recent review, see D. Cremer, P.v.R. Schleyer, N.L. Allinger, T. Clark, J. Gasteiger, P.A. Kollman, H.F. Schaefer, P.R. Schreiner III. (Eds.), Encyclopedia of Computational Chemistry, vol. 3, Wiley, Chichester, 1998, p. 1706.
[65] J. Cizek, Adv. Chem. Phys. 14 (1969) 35;
G.D. Purvis, R.J. Bartlett, J. Chem. Phys. 76 (1982) 1910;
J.A. Pople, M. Head-Gordon, K. Raghavachari, J. Chem. Phys. 87 (1987) 5968;
for a review on CC methods, see R.J. Bartlett, J. Phys. Chem. 93 (1989) 1697.
[66] R.J. Bartlett, in: P. Jørgensen, J. Simons (Eds.), Geometrical Derivatives of Energy Surfaces and Geometrical Properties, Reidel, Dordrecht, 1986;
J. Gauss, D. Cremer, Adv. Quant. Chem. 23 (1992) 205.
[67] R.D. Amos, Chem. Phys. Lett. 88 (1982) 89.
[68] M.S. Gordon, M.W. Schmidt, G.M. Chaban, K.R. Glaesemann, W.J. Stevens, C. Gonzalez, J. Chem. Phys. 110 (1999) 4199.
[69] R. Kurian, M. Filatov, J. Chem. Theory Comp. 4 (2008) 278.
[70] F. Pleiter, H. de Waard, Mössbauer Isomer Shifts (Ref. [6]), Chapter 5c.
[71] Z. Patyk, A. Baran, J.F. Berger, J. Dechargé, J. Dobaczewski, P. Ring, A. Sobiczewski, Phys. Rev. C 59 (1999) 704.
[72] R. Machleidt, Adv. Nucl. Phys. 19 (1989) 189.
[73] R. Machleidt, Phys. Rev. C 63 (2001) 024001.
[74] K.J. Duff, Phys. Rev. B 9 (1974) 66.
[75] W. Kündig, Hyperfine Interact. 2 (1976) 113.
[76] H. Backe, E. Kankeleit, H.K. Walter, Mössbauer Isomer Shifts (Ref. [6]), Chapter 14.
[77] Y. Zhang, J. Mao, E. Oldfield, J. Am. Chem. Soc. 124 (2002) 7829.
[78] R. Reschke, A. Trautwein, J.P. Desclaux, J. Phys. Chem. Solids 38 (1977) 837.
[79] A. Trautwein, F.E. Harris, A.J. Freeman, J.P. Desclaux, Phys. Rev. B 11 (1975) 4101.
[80] W.C. Nieuwpoort, D. Post, P.T. van Duijnen, Phys. Rev. B 17 (1978) 91.
[81] F. Neese, Inorg. Chim. Acta 337 (2002) 181.
[82] V.N. Nemykin, R.G. Hadt, Inorg. Chem. 45 (2006) 8297.
[83] J.C. Slater, K.H. Johnson, Phys. Rev. B 5 (1972) 844.

[84] M.L. De Siqueira, S. Larsson, W.D. Connolly, J. Phys. Chem. Solids 36 (1975) 1419.
[85] D. Guenzburger, D.M.S. Esquivel, J. Danon, Phys. Rev. B 18 (1978) 4561.
[86] D. Guenzburger, E.M.B. Saitovitch, M.A. De Paoli, H. Manela, J. Chem. Phys. 80 (1984) 735.
[87] O. Eriksson, A. Svane, J. Phys.: Condens. Matter 1 (1989) 1589.
[88] J. Terra, D. Guenzburger, Hyperfine Interact. 60 (1990) 627.
[89] J. Terra, D. Guenzburger, Phys. Rev. B 44 (1991) 8584.
[90] F. Neese, Curr. Opin. Chem. Biol. 7 (2003) 125.
[91] T. Lovell, J. Li, T. Liu, D.A. Case, L. Noodelman, J. Am. Chem. Soc. 123 (2001) 12392.
[92] T. Lovell, W.-G. Han, T. Liu, L. Noodelman, J. Am. Chem. Soc. 124 (2002) 5890.
[93] R. van Leeuwen, E.-J. Baerends, Phys. Rev. A 49 (1994) 2421.
[94] A.J.F. Boyle, P. Bunbury, C. Edwards, Proc. Phys. Soc. London 79 (1962) 416.
[95] V.A. Belyakov, Phys. Lett. 16 (1965) 279.
[96] J.P. Bocquet, Y.Y. Chu, O.C. Kistner, M.L. Perlman, G.T. Emery, Phys. Rev. Lett. 17 (1966) 809.
[97] K. Mazheika, D. Baltrunas, A. Dragunas, K. Makariunas, V. Remeikis, Lithuanian Phys. J. 38 (1998) 7.
[98] E. Antoncik, Hyperfine Interact. 8 (1980) 161.
[99] E. Antoncik, Phys. Rev. B 23 (1981) 6524.
[100] A. Svane, E. Antoncik, Phys. Rev. B 34 (1986) 1944.
[101] A. Svane, E. Antoncik, Phys. Rev. B 35 (1987) 4611.
[102] A. Svane, Phys. Rev. Lett. 60 (1988) 2693.
[103] J. Terra, D. Guenzburger, Phys. Rev. B 39 (1989) 50.
[104] J. Terra, D. Guenzburger, J. Phys. Condens. Matter 3 (1991) 6763.
[105] P.E. Lippens, Phys. Rev. B 60 (1999) 4576.
[106] P.E. Lippens, J. Olivier-Fourcade, J.C. Jumas, Hyperfine Interact. 126 (2000) 137.
[107] M. Devilers, J. Ladrière, Hyperfine Interact. 36 (1987) 101.
[108] T. Miura, Y. Hatsukawa, M. Yanaga, K. Endo, H. Nakahara, M. Fujioka, E. Tanaka, A. Hashizume, Hyperfine Interact. 28 (1986) 857.
[109] E. Hartmann, W. Winkler, Hyperfine Interact. 61 (1990) 1435.
[110] W.J.J. Spijkervet, F. Pleiter, Hyperfine Interact. 7 (1979) 285.
[111] J. Ladrière, M. Cogneau, A. Meykens, J. Phys. 41 (1980) Cl-131.
[112] P. Koran, Hyperfine Interact. 12 (1982) 1.
[113] P.R. Brady, J.F. Duncan, K.F. Mok, Proc. Roy. Soc. London Ser. A-Mater. Phys. Sci. 287 (1965) 343.
[114] J. Blomquist, B. Roos, M. Sundbom, J. Chem. Phys. 55 (1971) 141.
[115] J. Blomquist, B. Roos, M. Sundbom, Chem. Phys. Lett. 9 (1971) 160.
[116] A. Trautwein, F.E. Harris, Theor. Chim. Acta 30 (1973) 45.
[117] A. Trautwein, J.R. Regnard, F.E. Harris, Y. Maeda, Phys. Rev. B 7 (1973) 947.
[118] R. Reschke, A. Trautwein, Phys. Rev. B 15 (1977) 2708.
[119] J.P. Sanchez, J.M. Friedt, A. Trautwein, R. Reschke, Phys. Rev. B 19 (1979) 365.
[120] M. Grodzicki, V. Männing, A.X. Trautwein, J.M. Freidt, J. Phys. B: At. Mol. Phys. 20 (1987) 5595.
[121] W.H. Flygare, D.W. Hafemeister, J. Chem. Phys. 43 (1965) 789.
[122] A. Sawaryn, L.P. Aldridge, R. Bläs, V.R. Marathe, A.X. Trautwein, Hyperfine Interact. 29 (1986) 1303.
[123] A. Sadoc, R. Broer, C. de Graaf, Chem. Phys. Lett. 454 (2008) 196.
[124] V.N. Nemykin, N. Kobayashi, V.Y. Chernii, V.K. Belsky, Eur. J. Inorg. Chem. 2001 (2001) 733.
[125] Y. Zhang, E. Oldfield, J. Phys. Chem. B. 107 (2003) 7180.
[126] W.-G. Han, T. Lovell, T. Liu, L. Noodleman, Inorg. Chem. 42 (2003) 2751.
[127] T. Liu, T. Lovell, W.-G. Han, L. Noodleman, Inorg. Chem. 42 (2003) 5244.
[128] Y. Zhang, W. Gossman, E. Oldfield, J. Am. Chem. Soc. 125 (2003) 16387.
[129] J.C. Schoneboom, F. Neese, W. Thiel, J. Am. Chem. Soc. 127 (2005) 5840.
[130] W.-G. Han, T. Liu, T. Lovell, L. Noodleman, J. Am. Chem. Soc. 127 (2005) 15778.
[131] A. Svane, Phys. Rev. B 68 (2003) 064422.
[132] P.A. Flinn, Mössbauer Isomer Shifts (Ref. [6]), Chapter 9a;
S.L. Ruby, G.K. Shenoy, Mössbauer Isomer Shifts (Ref. [6]), Chapter 9b;
E.R. Bauminger, G.M. Kalvius, I. Nowik, Mössbauer Isomer Shifts (Ref. [6]), Chapter 10.
[133] V. Männing, M. Grodzicki, Theor. Chim. Acta 70 (1986) 189.
[134] M. Grodzicki, A.X. Trautwein, Hyperfine Interact. 29 (1986) 1547.
[135] W. Winkler, R. Vetter, E. Hartmann, Chem. Phys. 114 (1987) 347.
[136] M. Yanaga, K. Endo, H. Nakahara, S. Ikuta, T. Miura, M. Takahashi, M. Takeda, Hyperfine Interact. 62 (1990) 359.
[137] V.A. Varnek, A.A. Varnek, J. Struct. Chem. 38 (1997) 970.
[138] K. Jackson, S. Srinivas, J. Kortus, M. Pederson, Phys. Rev. B 65 (2002) 214201.
[139] A value, $\alpha = 0.26\alpha_0^3$ mm s$^{-1}$ obtained in the non-relativistic calculations in Ref. [138] has been corrected with relativistic scaling factor $S'(Z) = 2.306$ (see Ref. [40]).
[140] W.A. de Jong, J. Styszynski, L. Visscher, W.C. Nieuwpoort, J. Chem. Phys. 108 (1998) 5177.
[141] M. Pernpointner, M. Seth, P. Schwerdtfeger, J. Chem. Phys. 108 (1998) 6722.
[142] M. Pernpointner, L. Visscher, J. Chem. Phys. 114 (2001) 10389.
[143] P. Schwerdtfeger, T. Söhnel, M. Pernpointner, J.K. Laerdahl, F.E. Wagner, J. Chem. Phys. 115 (2001) 5913.
[144] G. Martìnez-Pinedo, P. Schwerdtfeger, E. Caurier, K. Langanke, W. Nazarewicz, T. Söhnel, Phys. Rev. Lett. 87 (2001) 062701.
[145] J.N.P. van Stralen, L. Visscher, J. Chem. Phys. 117 (2002) 3103.
[146] J.N.P. van Stralen, L. Visscher, Mol. Phys. 101 (2003) 2115.
[147] R.L.A. Haiduke, A.B.F. Da Silva, L. Visscher, J. Chem. Phys. 125 (2006) 064301.
[148] L. Belpassi, F. Tarantelli, A. Sgamelotti, H.M. Quiney, J.N.P. van Stralen, L. Visscher, J. Chem. Phys. 126 (2007) 064314.
[149] C.R. Jacob, L. Visscher, C. Thierfelder, P. Schwerdtfeger, J. Chem. Phys. 127 (2007) 204303.
[150] M. Filatov, D. Cremer, J. Chem. Phys. 121 (2004) 5618.
[151] I. Malkin, O.L. Malkina, V.G. Malkin, M. Kaupp, Chem. Phys. Lett. 396 (2004) 268.
[152] E. Malkin, I. Malkin, O.L. Malkina, V.G. Malkin, M. Kaupp, Phys. Chem. Chem. Phys. 8 (2006) 4079.